

# A Study of Slender Shapes of Minimum Drag Using the Newton-Busemann Pressure Coefficient Law<sup>†</sup>

ANGELO MIELE\*

*Boeing Scientific Research Laboratories*

## Summary

The problem of minimizing the drag of a slender, two-dimensional or axisymmetric body in hypersonic flow at zero angle of attack is considered under the assumption that the pressure coefficient law is Newton's impact law as modified by Busemann in order to include centripetal acceleration effects. After the condition that the pressure coefficient be nonnegative is accounted for and after arbitrary conditions are imposed on, in addition to the thickness and the length, the enclosed area and the moment of inertia of the contour in the two-dimensional case and the wetted area and the volume in the axisymmetric case, the minimal problem is formulated as a problem of the Mayer type and solved by the combined use of the Euler-Lagrange equations, the transversality condition, the Erdmann-Weierstrass corner condition, and the properties of the switching function.

Particular attention is devoted to the class of problems such that, among the four quantities being considered, two are prescribed while the remaining are free. For these problems, the extremal arc is composed of two subarcs: one is characterized by a positive pressure coefficient and is called the *regular shape*; the other is characterized by a zero pressure coefficient and is called the *free layer*. In this connection, the analysis shows the existence of two different types of solutions depending on whether the thickness is given or free.

If the thickness is given, the expression for the regular shape is a power law, and the transition from the regular shape to the free layer occurs in the second half of the body. In the two-dimensional case, the exponent of the power law is 1 if the length is given,  $3/2$  if the enclosed area is given, and 3 if the moment of inertia of the contour is given; the transition point from the power body to the free layer is located at 50 percent of the length if the length is given, at 66 percent if the enclosed area is given, and at 83 percent if the moment of inertia of the contour is given. In the axisymmetric case, the exponent of the power law is  $3/4$  if the length is given, 1 if the wetted area is given, and  $3/2$  if the volume is given; the transition point from the power body to the free layer is located at 60 percent of the length if the length is given, at 70 percent if the wetted area is given, and at 80 percent if the volume is given.

On the other hand, for problems where the thickness is free, the equation governing the regular shape is not that of a power body, and the point of transition to the free layer is located in the first half of the body. In the two-dimensional case, the transition point is at 28 percent of the length if the length and the en-

closed area are given, at 32 percent if the length and the moment of inertia of the contour are given, and at 45 percent if the enclosed area and the moment of inertia of the contour are given. In the axisymmetric case, the transition point is located at 35 percent of the length if the length and the wetted area are given, at 39 percent if the length and the volume are given, and at 46 percent if the wetted area and the volume are given.

For all of the cases considered, analytical expressions are obtained for the optimum shapes, the thickness ratios, and the drag coefficients.

## (1) Introduction

IN PREVIOUS PAPERS,<sup>1,2</sup> the problem of minimizing the drag of a slender body in a hypersonic, inviscid flow was considered under the assumption that the pressure coefficient law is that which results from Newton's impact theory. The results are necessarily limited and, hence, it is desirable to extend the analysis to include the effect of the curvature of the body in the streamwise direction.<sup>3-5</sup>

Since the pressure coefficient is due to the superposition of an impact term which depends on the slope only and a curvature term which depends on the ordinate as well as the curvature, one must expect the resulting optimum shapes to be generally different from those predicted by the simple impact theory. In addition, since the curvature term contains derivatives of higher order than the impact term, one must expect some complication of the boundary value problem, owing to the fact that the boundary conditions (either of the fixed end-point type or the natural type) involve not only the end-values of the abscissa and the ordinate but also the end-values of the slope. Hayes and Probstein were well aware of these difficulties<sup>6</sup> when they abandoned the indirect methods of the Calculus of Variations and proceeded to find the shape minimizing the drag for a given thickness and a given length by means of a rather unorthodox, partly analytical and partly intuitive, procedure. Actually, if the Mayer formulation is used and the condition that the pressure coefficient be nonnegative everywhere is accounted for, it is possible (a) to supply a rigorous justification of Hayes and Probstein's results by means of the indirect methods of the Calculus of Variations and (b) to extend their analysis to the more general case where, in addition to the thickness and the length, any number of conditions is imposed on the enclosed area and the moment of inertia of the contour in the two-dimensional

Received by IAS August 1, 1962. Revised and received November 19, 1962. To be presented at the IAS 31st Annual Meeting, New York, Jan. 21-23, 1963.

<sup>†</sup> This paper is a condensed version of the investigation presented in Refs. 3 and 4.

\* Director of Astrodynamics and Flight Mechanics.

The author is indebted to Prof. Julian Cole of California Institute of Technology for extremely helpful discussions. Also, he is indebted to Gary R. Saaris, Arthur H. Lusty, David G. Hull, and Robert E. Pritchard for analytical and numerical assistance.

case and on the wetted area and the volume in the axisymmetric case.

In the light of the above statement, an extensive investigation of optimum shapes in a hypersonic, inviscid flow has been undertaken, and analytical solutions have been obtained for a wide variety of bodies. The relevant results, which were originally summarized in Ref. 3 for the two-dimensional case and in Ref. 4 the axisymmetric case, are presented here under a unified treatment. After the general theory is developed, several particular cases are considered; they differ from each other because of the nature of the boundary conditions; in all of these cases, the end-values of the slope are free and must be determined from the solution of the variational problem.

## (2) Minimal Problem

For a slender body subjected to a hypersonic, inviscid flow, the Newton-Busemann pressure coefficient law is given by (Ref. 5)

$$C_p = 2\{\dot{y}^2 + [y\ddot{y}/(n+1)]\} \quad (1)$$

where  $x$  denotes a streamwise coordinate,  $y$  a normal coordinate, and the dot sign a derivative with respect to  $x$ . The numerical constant appearing in Eq. (1) has the value  $n = 0$  in the two-dimensional case and  $n = 1$  in the axisymmetric case. Consequently, if  $q$  denotes the dynamic pressure, if  $D$  denotes the drag (per unit span, in the two-dimensional case), and if reference is made to the portion of the body between stations 0 and  $x$ , the following relationships hold:

$$\left. \begin{array}{l} \text{Two-dimensional case} \\ D(x) = 4q \int_0^x (\dot{y}^3 + y\dot{y}\ddot{y})dx \\ \text{Axisymmetric case} \\ D(x) = 4\pi q \int_0^x \left( y\dot{y}^3 + \frac{y^2\dot{y}\ddot{y}}{2} \right) dx \end{array} \right\} \quad (2)$$

In addition, attention is focused on the following quantities: the area enclosed by the airfoil contour  $A$  and the moment of inertia of the contour  $M$  in the two-dimensional case; the wetted area  $S$  and the volume  $V$  in the axisymmetric case. These quantities are given by

$$\left. \begin{array}{l} \text{Two-dimensional case} \\ A(x) = 2 \int_0^x y dx \\ M(x) = 2 \int_0^x y^2 dx \\ \text{Axisymmetric case} \\ S(x) = 2\pi \int_0^x y dx \\ V(x) = \pi \int_0^x y^2 dx \end{array} \right\} \quad (3)$$

If  $s$  denotes the slope and  $c$  the curvature, if the definitions

Two-dimensional case

$$\left. \begin{array}{l} \alpha = D(x)/4q \\ \beta = A(x)/2 \\ \gamma = M(x)/2 \end{array} \right\}$$

Axisymmetric case

$$\left. \begin{array}{l} \alpha = D(x)/4\pi q \\ \beta = S(x)/2\pi \\ \gamma = V(x)/\pi \end{array} \right\} \quad (4)$$

are introduced, and if both sides of Eqs. (2) and (3) are differentiated with respect to the independent variable, the following differential constraints are obtained:

$$\left. \begin{array}{l} \varphi_1 \equiv \dot{\alpha} - y^n s^3 - [y^{n+1} s c / (n+1)] = 0 \\ \varphi_2 \equiv \dot{\beta} - y = 0 \\ \varphi_3 \equiv \dot{\gamma} - y^2 = 0 \\ \varphi_4 \equiv \dot{y} - s = 0 \\ \varphi_5 \equiv \dot{s} - c = 0 \end{array} \right\} \quad (5)$$

and enable one to treat the minimum drag problem as a problem of the Mayer type. After the requirement that the pressure coefficient be nonnegative everywhere is expressed as

$$\varphi_6 \equiv s^2 + [yc/(n+1)] - p^2 = 0 \quad (6)$$

where  $p$  denotes a *real* variable, it is seen that the differential system composed of Eqs. (5) and (6) involves one independent variable ( $x$ ), seven dependent variables ( $\alpha, \beta, \gamma, y, s, c, p$ ), and one degree of freedom. In this connection, after assuming that

$$x_i = \alpha_i = \beta_i = \gamma_i = y_i = 0 \quad (7)$$

and that some, but not all, of the remaining state variables are given at the end-points, one can formulate the minimum drag problem as follows: In the class of functions  $\alpha(x), \beta(x), \gamma(x), y(x), s(x), c(x), p(x)$  which are consistent with the differential constraints, Eqs. (5) and (6), and the initial conditions, Eq. (7), find that special set which minimizes the difference  $\Delta G = G_f - G_i$ , where  $G = \alpha$ .

## (3) Necessary Conditions

This problem is of the Mayer type with separated end-conditions. Consequently, after the Lagrange multipliers  $\lambda_1$  through  $\lambda_6$  are introduced, the extremal arc is described by the following Euler-Lagrange equations:<sup>9,10</sup>

$$\left. \begin{aligned}
 \dot{\lambda}_1 &= 0 \\
 \dot{\lambda}_2 &= 0 \\
 \dot{\lambda}_3 &= 0 \\
 \dot{\lambda}_4 &= -\lambda_1 n y^{n-1} s^3 - \lambda_1 y^n s c - \lambda_2 - \\
 &\quad 2\lambda_3 y + \frac{\lambda_6 c}{n+1} \\
 \dot{\lambda}_5 &= -3\lambda_1 y^n s^2 - \frac{\lambda_1 y^{n+1} c}{n+1} - \lambda_4 + 2\lambda_6 s \\
 0 &= -\frac{\lambda_1 y^{n+1} s}{n+1} - \lambda_5 + \frac{\lambda_6 y}{n+1} \\
 0 &= -2\lambda_6 p
 \end{aligned} \right\} \quad (8)$$

the first three of which can be integrated to give

$$\lambda_1 = C_1, \quad \lambda_2 = C_2, \quad \lambda_3 = C_3 \quad (9)$$

where  $C_1$  through  $C_3$  are constants. Furthermore, since the independent variable is not present in the constraining equations, the following first integral is valid:

$$C_1 \left( y^n s^3 + \frac{y^{n+1} s c}{n+1} \right) + C_2 y + C_3 y^2 + \lambda_4 s + \lambda_5 c = C \quad (10)$$

where  $C$  is a constant.

### (3.1) Discontinuous Solutions

As the seventh Euler equation indicates, the extremal arc is generally discontinuous and is composed of subarcs along which  $\lambda_6 = 0$  and subarcs along which  $p = 0$ . Along the former subarcs, which are called *regular shapes*, the pressure coefficient is positive as long as  $p$  is real. Along the latter subarcs, the pressure coefficient is zero as long as  $x > 0$ ; hence, these subarcs are called *free layers*.<sup>6</sup>

### (3.2) Corner Conditions

In the event that discontinuities are present, the Erdman-Weierstrass corner conditions must be applied. They require that the multipliers  $\lambda_4, \lambda_5$  be continuous at each corner point and that the integration constants  $C_1, C_2, C_3, C$  have the same value for all of the subarcs composing the extremal arc. Owing to the fact that the quantities  $y, s$  are continuous, inspection of the first integral, Eq. (10), shows that a discontinuity in the curvature is possible if, and only if,

$$\left( \frac{C_1 y^{n+1} s}{n+1} + \lambda_5 \right)_- = \left( \frac{C_1 y^{n+1} s}{n+1} + \lambda_5 \right)_+ = 0 \quad (11)$$

where the negative and positive signs denote conditions immediately before and after the corner point, respectively. If Eq. (11) is combined with the sixth Euler equation, it is apparent that, at a corner point,

$$(\lambda_6)_- = (\lambda_6)_+ = 0 \quad (12)$$

### (3.3) End-Conditions

The end-conditions are partly of the fixed end-point

type and partly of the natural type. The latter must be derived from the transversality condition

$$[-C dx + (C_1 + 1) d\alpha + C_2 d\beta + C_3 d\gamma + \lambda_4 dy + \lambda_5 ds]_i' = 0 \quad (13)$$

which is to be satisfied identically for all systems of differentials consistent with the prescribed end-conditions. If the initial and final values of the slope are free, the following general results are derived:

$$C_1 = -1, \quad \lambda_{5i} = \lambda_{5f} = 0 \quad (14)$$

the first of which, in combination with the first of Eqs. (9), implies that  $\lambda_1 = -1$  everywhere along the extremal arc.

An important class of problems is that in which, among the four quantities being considered (the semithickness  $d/2$ , the length  $l$ , the enclosed area  $A$ , and the moment of inertia of the contour  $M$  in the two-dimensional case; the semithickness, the length, the wetted area  $S$ , and the volume  $V$  in the axisymmetric case), two are prescribed while the remaining are free. For these problems, the transversality condition in combination with the sixth Euler equation and the first integral, Eq. (10), yields the relationships indicated in Table 1.

### (3.4) Legendre-Clebsch Condition

The application of the Legendre-Clebsch test to the present problem indicates that the drag is a minimum if the necessary condition  $\lambda_6 \leq 0$  is satisfied everywhere along the extremal arc.

### (3.5) Switching Function

From the previous discussion, it appears that the Lagrange multiplier  $\lambda_6$  plays a dominant role in determining the composition of the extremal arc and, for this reason, is called the *switching function*. After the sixth Euler equation is considered, the properties of this switching function can be summarized as follows:

$$\left. \begin{aligned}
 \lambda_6 &= 0, \quad \text{along the regular shape} \\
 \lambda_6 &\leq 0, \quad \text{along the free layer} \\
 \lambda_{60} &= 0, \quad \text{at a corner point } 0 \\
 \lambda_{6f} &= -y_f^n \dot{y}_f, \quad \text{at the final point } F
 \end{aligned} \right\} \quad (15)$$

## (4) Solution Process

In the previous sections, it has been shown that the extremal arc is discontinuous and is composed of regular shapes and free layers. Here, the different subarcs are investigated in detail, and a general condition for transition is derived.

### (4.1) Regular Shape

If the condition  $\lambda_6 = 0$  is combined with the fifth and sixth Euler equations, the following expressions are obtained for the remaining Lagrange multipliers:

$$\lambda_4 = 2y^n \dot{y}^2, \quad \lambda_5 = \frac{y^{n+1} \dot{y}}{(n+1)} \quad (16)$$

Consequently, the first integral (10) reduces to

$$y^n \dot{y}^3 + C_2 y + C_3 y^2 = C \quad (17)$$

This means that the general equation of the regular shape is given by

$$x = \int \sqrt{\frac{y^n}{C - C_2 y - C_3 y^2}} dy + \text{const.} \quad (18)$$

and, except for the integration constant, is formally identical to the equation derived using the simple Newtonian expression for the pressure coefficient.<sup>1, 2</sup>

#### (4.2) Free Layer

If the condition  $p = 0$  is combined with the sixth constraining equation, it is seen that the differential equation governing a free layer is

$$\dot{y}^2 + [y\ddot{y}/(n+1)] = 0 \quad (19)$$

and admits the first integral

$$y^{n+1} \dot{y} = \text{const.} \quad (20)$$

as well as the second integral

$$y = (C_4 x + C_5)^{1/(n+2)} \quad (21)$$

where  $C_4$  and  $C_5$  are constants.

For the free layer, it is of fundamental interest to evaluate the distribution of the switching function. To do so, the sixth Euler-Lagrange equation yields

$$\lambda_6 = (n+1)(\lambda_5/y) - y^n \dot{y} \quad (22)$$

which implies that

$$\dot{\lambda}_6 = \frac{n+1}{y} \dot{\lambda}_5 - (n+1) \frac{\lambda_5}{y^2} \dot{y} - n y^{n-1} \dot{y}^2 - y^n \ddot{y} \quad (23)$$

Consequently, use of the fifth Euler-Lagrange equation in combination with Eqs. (10), (19), and (22) leads to the following expression for the derivative of the switching function:

$$\dot{\lambda}_6 = n \frac{\dot{y}}{y} \lambda_6 + \frac{n+1}{y \dot{y}} (y^n \dot{y}^3 - C + C_2 y + C_3 y^2) \quad (24)$$

After denoting with the subscript  $o$  quantities evaluated at the beginning of the free layer and observing that

$$y^{n+1} \dot{y} = y_0^{n+1} \dot{y}_0, \quad \dot{\lambda}_6 = (d\lambda_6/dy) \dot{y} \quad (25)$$

one can rewrite Eq. (24) in the form

$$d\left(\frac{\lambda_6}{y^n}\right) = \frac{n+1}{(y_0^{n+1} \dot{y}_0)^2} \left[ \frac{(y_0^{n+1} \dot{y}_0)^3}{y^{n+2}} - C y^{n+1} + C_2 y^{n+2} + C_3 y^{n+3} \right] dy \quad (26)$$

whose general integral is

$$\frac{\lambda_6}{y^n} = \frac{n+1}{(y_0^{n+1} \dot{y}_0)^2} \left[ -\frac{(y_0^{n+1} \dot{y}_0)^3}{(n+1)y^{n+1}} - C \frac{y^{n+2}}{n+2} + C_2 \frac{y^{n+3}}{n+3} + C_3 \frac{y^{n+4}}{n+4} \right] + \text{const.} \quad (27)$$

This equation, in combination with the initial conditions

$$\lambda_{60} = 0, \quad y_0^n \dot{y}_0^3 - C + C_2 y_0 + C_3 y_0^2 = 0 \quad (28)$$

determines the distribution of the switching function along the free layer and is of fundamental importance in determining the composition of the extremal arc, as is shown in the following analysis.

#### (4.3) Sequence of Subarcs

The next step is to determine the proper sequence of subarcs. It is clear that the extremal arc cannot start with a free layer: the pressure coefficient would be zero everywhere except at the origin where a singularity would occur and, in the slender body approximation, would produce an infinitely large drag.<sup>5</sup> If it is assumed that the extremal arc starts with a regular shape, the next question is to investigate (a) whether a transition to a free layer may occur and (b) in the affirmative case, whether a further transition back to a regular shape is possible.

The second part of the question formulated above is now investigated by examining the distribution of the switching function along the free layer with the aid of Eqs. (27) and (28). Since the conclusions depend on the boundary conditions, the analysis will be restricted to the class of problems considered in Table 1, that is, problems where two of the four quantities being considered (the thickness, the length, the enclosed area, and the moment of inertia of the contour in the two-dimensional case; the thickness, the length, the wetted area, and the volume in the axisymmetric case) are prescribed while the remaining are free. Consider, for

TABLE 1. Boundary Conditions

Quantities given									Additional relationships
Two-dimensional case	Axisymmetric case	$C_1$	$C_2$	$C_3$	$C$	$\lambda_{4f}$	$\lambda_{5f}$	$\lambda_{6f}$	
$d, l$	$d, l$	-1	0	0			0	0	
$d, A$	$d, S$	-1		0	0		0	0	
$d, M$	$d, V$	-1	0		0		0	0	
$l, A$	$l, S$	-1		0		0	0	0	$C_2(d/2) = C$
$l, M$	$l, V$	-1	0			0	0	0	$C_3(d/2)^2 = C$
$A, M$	$S, V$	-1			0	0	0	0	$C_2 + C_3(d/2) = 0$

TABLE 2. Solutions of the Transition Equation (Two-Dimensional Problem)

Quantities given	End-conditions	Transition equation	$\eta_0$	$\xi_0$
$d, l$	$K_2 = K_3 = 0$	$3\eta_0^2 - 1 = 0$	0.577	0.500
$d, A$	$K_1 = K_3 = 0$	$4\eta_0^3 - 1 = 0$	0.630	0.664
$d, M$	$K_1 = K_2 = 0$	$5\eta_0^4 - 1 = 0$	0.669	0.829
$l, A$	$K_3 = 0, K_1 - K_2 = 0$	$8\eta_0^3 - 9\eta_0^2 + 1 = 0$	0.422	0.281
$l, M$	$K_2 = 0, K_1 - K_3 = 0$	$5\eta_0^4 - 6\eta_0^2 + 1 = 0$	0.447	0.322
$A, M$	$K_1 = 0, K_2 + K_3 = 0$	$15\eta_0^4 - 16\eta_0^3 + 1 = 0$	0.486	0.446

instance, the first of these problems—that in which the thickness and the length are prescribed. The transversality condition yields  $C_2 = C_3 = 0$  and, as a consequence, Eqs. (27) and (28) can be combined to give the relationship

$$\frac{\lambda_6}{y^n y_0} = \frac{2n+3}{n+2} - \left(\frac{y_0}{y}\right)^{n+1} - \frac{n+1}{n+2} \left(\frac{y}{y_0}\right)^{n+2} \quad (29)$$

Hence, for every  $y > y_0$ , the switching function satisfies the inequality  $\lambda_6 < 0$  so that no transition from the free layer back to the regular shape is possible. Since an analogous result can be shown to hold for each of the cases considered in Table 1 (as long as the inequality constraint relative to the pressure coefficient is satisfied at every point of the regular shape preceding the free layer), the following conclusion is reached: For the class of two-dimensional problems involving the thickness, the length, the enclosed area, and the moment of inertia of the contour and for the class of axisymmetric problems involving the thickness, the length, the wetted area, and the volume such that any two of these quantities are prescribed while the remaining two are free, multiple transitions must be excluded. This means that the extremal arc includes at most two subarcs, that is, a regular shape and a free layer.\*

After it has been concluded that, for the problems considered here, the maximum number of subarcs is two, the next step is to determine (a) whether the extremal arc consists of a regular shape only or of a regular shape followed by a free layer and (b) in the latter case, what the coordinates of the transition point are. In order to answer these questions, it will be hypothetically assumed that the entire extremal arc is composed of a regular shape starting at the origin and a free layer terminating at the final point. If the subscripts  $o$  and  $f$  denote quantities evaluated at the beginning and at the end of the free layer, respectively, and if the boundary conditions

$$\lambda_{6o} = 0, \quad \lambda_{6f} = -\frac{y_0^{n+1} \dot{y}_0}{d/2} \quad (30)$$

are considered, use of Eq. (27) yields the relationship

\* For the particular case in which the thickness and the length are given, this conclusion had already been arrived at by Gonor,<sup>8</sup> who thereby supported the previous findings of Hayes and Probst.<sup>6</sup> Gonor's analysis was limited to the class of bodies involving at most two subarcs. Thus, while his proof is interesting, it is less general than that contained herein.

$$\left(\frac{y_0}{d/2}\right)^{n+1} \dot{y}_0 + \frac{n+1}{(y_0^{n+1} \dot{y}_0)^2} \left[ -\frac{(y_0^{n+1} \dot{y}_0)^3}{(n+1)y^{n+1}} - C \frac{y^{n+2}}{n+2} + C_2 \frac{y^{n+3}}{n+3} + C_3 \frac{y^{n+4}}{n+4} \right]^{d/2}_{y_0} = 0 \quad (31)$$

Furthermore, if the definitions

$$K_1 = C(d/2)^{-n}, \quad K_2 = C_2(d/2)^{1-n}, \quad K_3 = C_3(d/2)^{2-n} \quad (32)$$

are introduced in combination with the dimensionless ordinate  $\eta = 2y/d$ , Eq. (31) becomes

$$K_3 \frac{n+1}{n+4} \eta_0^{2n+5} + K_2 \frac{n+1}{n+3} \eta_0^{2n+4} - K_1 \frac{n+1}{n+2} \eta_0^{2n+3} - \left( K_3 \frac{n+1}{n+4} + K_2 \frac{n+1}{n+3} - K_1 \frac{n+1}{n+2} \right) \eta_0^{n+1} - \dot{y}_f^3 = 0 \quad (33)$$

where  $\dot{y}_f$  denotes the slope of the extremal arc at the final point. If the second of Eqs. (28) is rewritten in the dimensionless form

$$K_3 \eta_0^{2n+5} + K_2 \eta_0^{2n+4} - K_1 \eta_0^{2n+3} + \dot{y}_f^3 = 0 \quad (34)$$

and if the slope at the final point is eliminated from Eqs. (33) and (34), one obtains the fundamental transition equation

$$K_3 \frac{2n+5}{n+4} \eta_0^{n+4} + K_2 \frac{2n+4}{n+3} \eta_0^{n+3} - K_1 \frac{2n+3}{n+2} \eta_0^{n+2} - \left( K_3 \frac{n+1}{n+4} + K_2 \frac{n+1}{n+3} - K_1 \frac{n+1}{n+2} \right) = 0 \quad (35)$$

whose solution determines the ordinate of the transition point. With the aid of this equation, one can exclude the possibility of solutions composed of a regular shape only. In fact, should solutions of this type exist, then Eq. (35) would reduce to

$$K_3 + K_2 - K_1 = 0 \quad (36)$$

Now, for problems where the thickness is given, only two of these constants are zero so that Eq. (36) cannot be satisfied. On the other hand, for problems where the thickness is free, the constants  $K_1, K_2, K_3$  are such that Eq. (36) is satisfied (see Tables 2 and 3). However, because of Eq. (34), the slope of the solution at the final point would be  $\dot{y}_f = 0$  and the pressure coef-

ficient would reduce to  $2y_f\ddot{y}_f/(n+1)$ . Since the resulting regular shape would exhibit a negative curvature in the neighborhood of the final point, the pressure coefficient would be negative, thus violating the basic inequality constraint of the problem. In conclusion, for the problems considered in Table 1, there exist no solutions of the form  $\eta_0 = 1$ ; this means that, in all cases, the extremal arc starts with a regular shape and ends with a free layer.

#### (4.4) Properties of the Extremal Arc

After the transition point has been determined, Eqs. (18) and (21) in combination with the appropriate end-conditions, yield the following equations for the regular shape:

$$\frac{\xi}{\xi_0} = \frac{\int_0^{\eta_0} \sqrt{\frac{\eta^n}{K_1 - K_2\eta - K_3\eta^2}} d\eta}{\int_0^{\eta_0} \sqrt{\frac{\eta^n}{K_1 - K_2\eta - K_3\eta^2}} d\eta} \quad (37)$$

and the free layer:

$$(\xi - 1)/(\xi_0 - 1) = (\eta^{n+2} - 1)/(\eta_0^{n+2} - 1) \quad (38)$$

in which  $\xi = x/l$  denotes the dimensionless abscissa of the generic point and  $\xi_0$  the dimensionless abscissa of the transition point. The latter must be determined in the light of the continuity requirement for the slopes at the transition point and is given by

$$\xi_0 = 1/(1 + K_0) \quad (39)$$

where

$$K_0 = \frac{(1 - \eta_0^{n+2}) \sqrt{\frac{\eta_0^n}{K_1 - K_2\eta_0 - K_3\eta_0^2}}}{(n+2)\eta_0^{n+1} \int_0^{\eta_0} \sqrt{\frac{\eta^n}{K_1 - K_2\eta - K_3\eta^2}} d\eta} \quad (40)$$

Once the shape is known, the following dimensionless integrals can be evaluated:

$$\left. \begin{aligned} I_D &= \int_0^{\xi_0} \left( \eta^n \dot{\eta}^3 + \frac{\eta^{n+1} \ddot{\eta}}{n+1} \right) d\xi = \\ &\quad \left[ \frac{\eta^{n+1} \dot{\eta}^2}{2(n+1)} \right]_0^{\xi_0} + \frac{1}{2} \int_0^{\xi_0} \eta^n \dot{\eta}^3 d\xi \\ I_A &= I_S = \int_0^1 \eta d\xi, \quad I_M = I_V = \int_0^1 \eta^2 d\xi \end{aligned} \right\} \quad (41)$$

They are tied to the corresponding dimensional quantities by the relationships

$$\left. \begin{aligned} \text{Two-dimensional case} \\ D &= (qd^3/2l^2)I_D \\ A &= dl I_A \\ M &= (d^2l/2)I_M \\ \text{Axisymmetric case} \\ D &= (\pi qd^4/4l^2)I_D \\ S &= \pi dl I_S \\ V &= (\pi d^2l/4)I_V \end{aligned} \right\} \quad (42)$$

In this way, it is possible to express every unknown quantity in terms of given quantities and the dimensionless integrals, Eqs. (41). Incidentally, if the thickness ratio is defined as  $\tau = d/l$  and if the drag coefficient is referred to the frontal area at  $x = l$ , the following relationship can be readily established between the drag coefficient and the thickness ratio:

$$C_D = [I_D/(2 - n)]\tau^2 \quad (43)$$

### (5) Two-Dimensional Problem

In the previous section, the minimum drag problem was solved in general for arbitrary boundary conditions. Here, several particular cases associated with the two-dimensional problem ( $n = 0$ ) are considered, and the corresponding extremal arcs are calculated. Then, the results are summarized in Fig. 1 and Tables 2 and 4.

#### (5.1) Given Thickness and Length

If the thickness and the length are given while the enclosed area and the moment of inertia of the contour are free, the transversality condition leads to  $C_2 = C_3 = 0$ , which imply that  $K_2 = K_3 = 0$ . Consequently, the transition equation (35) in combination with Eqs. (39) and (40) yields the following coordinates for the transition point (Table 2):

$$\xi_0 = 1/2, \quad \eta_0 = 1/\sqrt{3} \quad (44)$$

Furthermore, Eqs. (37) and (38) yield the following expressions for the regular shape:

$$\eta/\eta_0 = \xi/\xi_0 \quad (45)$$

and the free layer:

TABLE 3. Solutions of the Transition Equation (Axisymmetric Problem)

Quantities given	End-conditions	Transition equation	$\eta_0$	$\xi_0$
$d, l$	$K_2 = K_3 = 0$	$5\eta_0^3 - 2 = 0$	0.737	0.600
$d, S$	$K_1 = K_3 = 0$	$3\eta_0^4 - 1 = 0$	0.760	0.701
$d, V$	$K_1 = K_2 = 0$	$7\eta_0^5 - 2 = 0$	0.778	0.801
$l, S$	$K_3 = 0, K_1 - K_2 = 0$	$9\eta_0^4 - 10\eta_0^3 + 1 = 0$	0.602	0.350
$l, V$	$K_2 = 0, K_1 - K_3 = 0$	$21\eta_0^5 - 25\eta_0^3 + 4 = 0$	0.617	0.385
$S, V$	$K_1 = 0, K_2 + K_3 = 0$	$14\eta_0^5 - 15\eta_0^4 + 1 = 0$	0.637	0.463

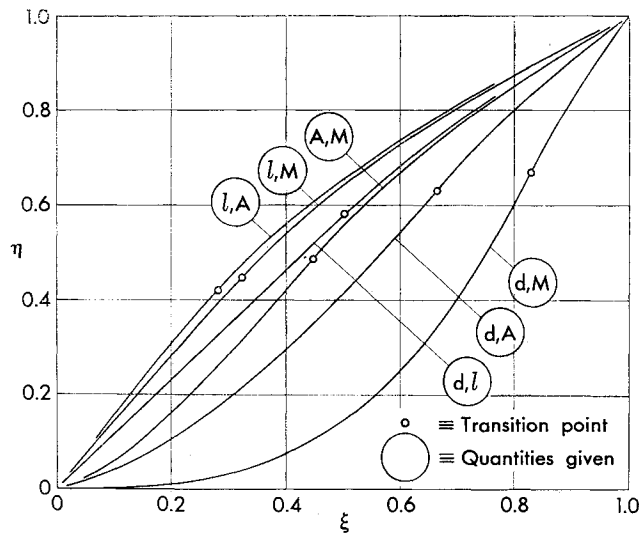


FIG. 1. Optimum two-dimensional bodies.

$$\eta = \sqrt{1 - [(1 - \eta_0^2)/(1 - \xi_0)](1 - \xi)} \quad (46)$$

In conclusion, the body having the minimum drag for a given thickness and a given length is a wedge followed by a free layer with the transition point at mid-length. In this way, a rigorous justification is given of the results presented by Hayes and Probstein.<sup>6</sup> Once the shape is known, the dimensionless integrals (41) as well as the enclosed area, the moment of inertia of the contour, and the minimum drag can be determined (Table 4). In particular, the drag coefficient of the optimum body must be calculated using Eq. (43) and is given by

$$C_D = (2/3\sqrt{3})\tau^2 \quad (47)$$

where  $\tau = d/l$  is the thickness ratio. Incidentally, this drag coefficient as well as the associated drag do not change if the free layer is replaced by any body surface lying inside of it.<sup>6</sup> However, this may not necessarily be true in the other cases analyzed in the following sections.

### (5.2) Given Thickness and Enclosed Area

If the thickness and the enclosed area are given while

the length and the moment of inertia of the contour are free, the transversality condition leads to  $C = C_3 = 0$ , which imply that  $K_1 = K_3 = 0$ . Consequently, the transition equation leads to the following coordinates for the transition point:

$$\xi_0 = \frac{3}{2(1 + \sqrt[3]{2})}, \quad \eta_0 = \frac{1}{\sqrt[3]{4}} \quad (48)$$

Since the equation of the regular shape is given by

$$\eta/\eta_0 = (\xi/\xi_0)^{3/2} \quad (49)$$

one concludes that the shape minimizing the drag for a given thickness and a given enclosed area is a 3/2-power body followed by a free layer with the transition point at 66 percent of the length. The thickness ratio of this body and the associated drag coefficient are given by

$$\left. \begin{aligned} \tau &= \frac{4}{5} \frac{\sqrt[3]{2}}{1 + \sqrt[3]{2}} \frac{d^2}{A} \\ C_D &= \frac{(1 + \sqrt[3]{2})^2}{10} \tau^2 \end{aligned} \right\} \quad (50)$$

### (5.3) Given Thickness and Moment of Inertia of the Contour

If the thickness and the moment of inertia of the contour are given while the length and the enclosed area are free, the transversality condition leads to  $C = C_2 = 0$ , which imply that  $K_1 = K_2 = 0$ . Consequently, the following coordinates can be determined for the transition point:

$$\xi_0 = 6/(5 + \sqrt{5}), \quad \eta_0 = 1/\sqrt[4]{5} \quad (51)$$

Since the equation of the regular shape is given by

$$\eta/\eta_0 = (\xi/\xi_0)^3 \quad (52)$$

it is concluded that the contour of the optimum body is a cubic followed by a free layer with the transition point at 83 percent of the length. The thickness ratio of this body and the associated drag coefficient are given by

TABLE 4. Optimum Two-Dimensional Bodies

Quantities given	$d$	$l$	$\tau$	$A$	$M$	$\frac{D}{q}$	$\frac{C_D}{\tau^2}$
$d, l$	$d$	$l$	$\frac{d}{l}$	$0.548 dl$	$0.194 d^2 l$	$0.385 \frac{d^3}{l^2}$	0.385
$d, A$	$d$	$2.242 \frac{A}{d}$	$0.446 \frac{d^2}{A}$	$A$	$0.337 dA$	$0.102 \frac{d^5}{A^2}$	0.511
$d, M$	$d$	$11.33 \frac{M}{d^2}$	$0.0883 \frac{d^3}{M}$	$3.206 \frac{M}{d}$	$M$	$0.0109 \frac{d^7}{M^2}$	1.398
$l, A$	$1.667 \frac{A}{l}$	$l$	$1.667 \frac{A}{l^2}$	$A$	$0.612 \frac{A^2}{l}$	$2.002 \frac{A^3}{l^5}$	0.432
$l, M$	$2.160 \sqrt{\frac{M}{l}}$	$l$	$2.160 \sqrt{\frac{M}{l^3}}$	$1.268 \sqrt{Ml}$	$M$	$4.138 \sqrt{\frac{M^3}{l}}$	0.410
$A, M$	$2.800 \frac{M}{A}$	$0.688 \frac{A^2}{M}$	$4.069 \frac{M^2}{A^3}$	$A$	$M$	$19.62 \frac{M^5}{A^7}$	0.423

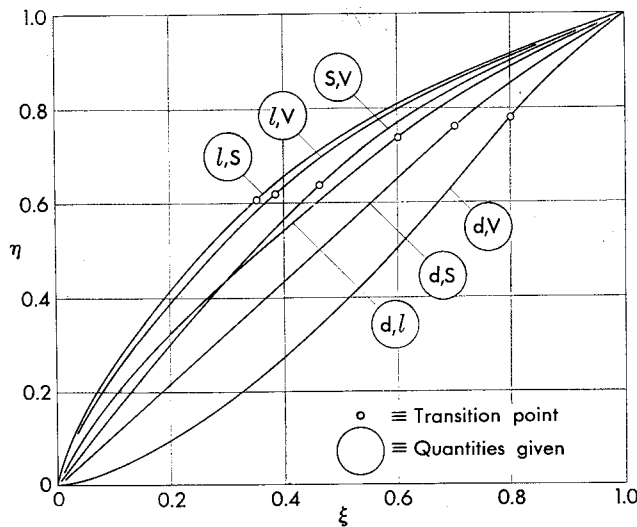


FIG. 2. Optimum axisymmetric bodies.

$$\tau = \frac{\sqrt{5} - 1}{14} \frac{d^3}{M}, \quad C_D = \frac{5\sqrt{5}}{28} (3 + \sqrt{5}) \tau^2 \quad (53)$$

#### (5.4) Given Length and Enclosed Area

If the length and the enclosed area are given while the thickness and the volume are free, the transversality condition leads to  $C_3 = 0$ ,  $\lambda_{4f} = 0$ , which imply that  $K_3 = 0$ ,  $K_1 = K_2$ . Consequently, the solution of the transition equation yields the following coordinates for the transition point:

$$\xi_0 = 0.281, \quad \eta_0 = (1 + \sqrt{33})/16 \quad (54)$$

Furthermore, use of Eq. (37) leads to the following expression for the regular shape:

$$\xi/\xi_0 = [1 - (1 - \eta)^{2/3}] / [1 - (1 - \eta_0)^{2/3}] \quad (55)$$

Finally, the expressions for the thickness ratio and the drag coefficient become

$$\tau = 1.667(A/l^3), \quad C_D = 0.432\tau^2 \quad (56)$$

#### (5.5) Given Length and Moment of Inertia of the Contour

If the length and the moment of inertia of the contour

are prescribed while the thickness and the enclosed area are free, the transversality condition leads to  $C_2 = 0$ ,  $\lambda_{4f} = 0$ , which imply that  $K_2 = 0$ ,  $K_1 = K_3$ . Consequently, the transition equation is solved by

$$\xi_0 = 0.322, \quad \eta_0 = 1/\sqrt{5} \quad (57)$$

The regular shape is described by the equation

$$\xi/\xi_0 = f(\eta)/f(\eta_0) \quad (58)$$

where

$$f(\eta) = \frac{\eta}{\sqrt{3} + 1 - \sqrt[3]{1 - \eta^2}} + \frac{\sqrt{3} - 1}{2\sqrt[3]{3}} F(\varphi, k) - \sqrt[3]{3} E(\varphi, k) \quad (59)$$

and where the symbols  $F$  and  $E$  denote the incomplete elliptic integrals of the first and second kind, whose argument  $\varphi$  and parameter  $k$  are defined as

$$\left. \begin{aligned} \varphi &= \arccos \frac{\sqrt{3} - 1 + \sqrt[3]{1 - \eta^2}}{\sqrt{3} + 1 - \sqrt[3]{1 - \eta^2}} \\ k &= \sqrt{(2 + \sqrt{3})/4} \end{aligned} \right\} \quad (60)$$

The thickness ratio of this shape and the associated drag coefficient are given by

$$\tau = 2.160 \sqrt{M/l^3}, \quad C_D = 0.410 \tau^2 \quad (61)$$

#### (5.6) Given Enclosed Area and Moment of Inertia of the Contour

If the enclosed area and the moment of inertia of the contour are prescribed while the thickness and the length are free, the transversality condition leads to  $C = 0$ ,  $\lambda_{4f} = 0$ , which imply that  $K_1 = 0$ ,  $K_2 + K_3 = 0$ . Consequently, solution of the transition equation yields the following coordinates for the transition point:

$$\xi_0 = 0.446, \quad \eta_0 = 0.486 \quad (62)$$

The regular shape minimizing the drag is described by the relationship

$$\frac{\xi}{\xi_0} = \frac{g(\eta) - g(0)}{g(\eta_0) - g(0)} \quad (63)$$

where

TABLE 5. Optimum Bodies of Revolution

Quantities given	$d$	$l$	$\tau$	$A$	$M$	$\frac{D}{q}$	$\frac{C_D}{\tau^2}$
$d, l$	$d$	$l$	$d/l$	$1.901 dl$	$0.348 d^2 l$	$0.226 \frac{d^4}{l^2}$	0.288
$d, S$	$d$	$0.598 \frac{S}{d}$	$1.673 \frac{d^2}{S}$	$S$	$0.175 dS$	$0.746 \frac{d^8}{S^2}$	0.339
$d, V$	$d$	$4.500 \frac{V}{d^2}$	$0.222 \frac{d^3}{V}$	$6.056 \frac{V}{d}$	$V$	$0.0219 \frac{d^8}{V^2}$	0.564
$l, S$	$0.477 \frac{S}{l}$	$l$	$0.477 \frac{S}{l^2}$	$S$	$0.0919 \frac{S^2}{l}$	$0.0139 \frac{S^4}{l^6}$	0.342
$l, V$	$1.596 \sqrt{\frac{V}{l}}$	$l$	$1.596 \sqrt{\frac{V}{l^3}}$	$3.280 \sqrt{lV}$	$V$	$1.632 \frac{V^2}{l^4}$	0.321
$S, V$	$5.333 \frac{V}{S}$	$0.0980 \frac{S^2}{V}$	$54.45 \frac{V^2}{S^3}$	$S$	$V$	$20,325 \frac{V^6}{S^8}$	0.307



$$g(\eta) = \frac{2\eta - 1}{\sqrt{3} + 1 - \sqrt[3]{4\eta(1-\eta)}} - \frac{\sqrt{3} - 1}{2\sqrt[3]{3}} \times F(\varphi, k) + \sqrt[3]{3} E(\varphi, k) \quad (64)$$

and where the argument and the parameter of the elliptic integrals are given by

$$\left. \begin{aligned} \varphi &= \arccos \frac{\sqrt{3} - 1 + \sqrt[3]{4\eta(1-\eta)}}{\sqrt{3} + 1 - \sqrt[3]{4\eta(1-\eta)}} \\ k &= \sqrt{(2 + \sqrt{3})/4} \end{aligned} \right\} \quad (65)$$

The thickness ratio of this shape and the associated drag coefficient are given by

$$\tau = 4.069(M^2/A^3), \quad C_D = 0.423\tau^2 \quad (66)$$

### (6) Axisymmetric Problem

In this section, several particular cases associated with the axisymmetric problem ( $n = 1$ ) are considered, and the associated extremal arcs are calculated. Then, the results are summarized in Fig. 2 and Tables 3 and 5.

#### (6.1) Given Thickness and Length

If the thickness and the length are given while the wetted area and the volume are free, the transversality condition leads to  $K_2 = K_3 = 0$ . Consequently, the transition equation, Eq. (35), in combination with Eqs. (39) and (40) yields the following coordinates for the transition point (Table 3):

$$\xi_0 = 3/5, \quad \eta_0 = \sqrt[3]{2/5} \quad (67)$$

Furthermore, Eqs. (37) and (38) yield the following expressions for the regular shape:

$$\eta/\eta_0 = (\xi/\xi_0)^{3/4} \quad (68)$$

and the free layer:

$$\eta = \sqrt[3]{1 - \frac{1 - \eta_0^3}{1 - \xi_0} (1 - \xi)} \quad (69)$$

In conclusion, the contour of minimum drag for a given thickness and a given length is a 3/4-power body followed by a free layer with the transition point at 60 percent of the length. Once more, a rigorous justification is given of the results presented by Hayes and Probst.<sup>6</sup> The drag coefficient of the optimum body must be calculated using Eq. (43) and is given by

$$C_D = (25/64)\sqrt[3]{2/5}\tau^2 \quad (70)$$

where  $\tau = d/l$  is the thickness ratio.

#### (6.2) Given Thickness and Wetted Area

If the thickness and the wetted area are given while the length and the volume are free, the transversality condition leads to  $K_1 = K_3 = 0$ . Consequently, the transition equation leads to the following coordinates for the transition point:

$$\xi_0 = \frac{3\sqrt[3]{3}}{2\sqrt[3]{3} + 3}, \quad \eta_0 = \frac{1}{\sqrt[3]{3}} \quad (71)$$

Since the equation of the regular shape is given by

$$\eta/\eta_0 = \xi/\xi_0 \quad (72)$$

one concludes that the shape minimizing the drag for a given thickness and a given enclosed area is a cone followed by a free layer with the transition point at 70 percent of the length. The thickness ratio of this body and the associated drag coefficient are given by

$$\tau = \frac{3\pi}{2\sqrt[3]{3} + 3} \frac{d^2}{S}, \quad C_D = \frac{(2\sqrt[3]{3} + 3)^2}{54\sqrt{3}} \tau^2 \quad (73)$$

#### (6.3) Given Thickness and Volume

If the thickness and the volume are given while the length and the wetted area are free, the transversality condition leads to  $K_1 = K_2 = 0$ . Consequently, the following coordinates can be determined for the transition point:

$$\xi_0 = \frac{9}{7} \frac{\sqrt[5]{392}}{\sqrt[5]{392} + 2}, \quad \eta_0 = \sqrt[5]{\frac{2}{7}} \quad (74)$$

Since the equation of the regular shape is given by

$$\eta/\eta_0 = (\xi/\xi_0)^{3/2} \quad (75)$$

it is concluded that the contour of the optimum shape is a 3/2-power body followed by a free layer with the transition point at 80 percent of the length. The thickness ratio and the drag coefficient of this body are given by

$$\left. \begin{aligned} \tau &= \frac{3\pi}{8(\sqrt[5]{392} + 2)} \frac{d^3}{V} \\ C_D &= \frac{49}{288} \sqrt[5]{\frac{7}{2}} \left( \frac{\sqrt[5]{392} + 2}{\sqrt[5]{392}} \right)^2 \tau^2 \end{aligned} \right\} \quad (76)$$

#### (6.4) Given Length and Wetted Area

If the length and the wetted area are given while the thickness and the volume are free, the transversality condition leads to  $K_3 = 0$ ,  $K_1 = K_2$ . Consequently, the solution of the transition equation yields the following coordinates for the transition point:

$$\xi_0 = 0.350, \quad \eta_0 = 0.602 \quad (77)$$

Furthermore, use of Eq. (37) leads to the following expression for the regular shape:

$$\xi/\xi_0 = f(\eta)/f(\eta_0) \quad (78)$$

where

$$\begin{aligned} f(\eta) &= -\sqrt[3]{\eta(1-\eta)^2} + \frac{1}{2} \log(\sqrt[3]{\eta} + \sqrt[3]{1-\eta}) + \\ &\quad \frac{1}{\sqrt{3}} \arctan \frac{\sqrt{3}\sqrt[3]{\eta}}{2\sqrt[3]{1-\eta} - \sqrt[3]{\eta}} \end{aligned} \quad (79)$$

Finally, the expressions for the thickness ratio and the drag coefficient become

$$\tau = 0.477(S/l^2), \quad C_D = 0.342\tau^2 \quad (80)$$

### (6.5) Given Length and Volume

If the length and the volume are prescribed while the thickness and the wetted area are free, the transversality condition leads to  $K_2 = 0$ ,  $K_1 = K_3$ . Consequently, the transition equation is solved by

$$\xi_0 = 0.385, \quad \eta_0 = 0.617 \quad (81)$$

The regular shape is described by the equation

$$\frac{\xi}{\xi_0} = \frac{h(\eta) - h(0)}{h(\eta_0) - h(0)} \quad (82)$$

where

$$\eta = \frac{2\eta^2 - 1}{\sqrt{3} + 1 - \sqrt[3]{4\eta^2(1 - \eta^2)}} - \frac{\sqrt{3} - 1}{2\sqrt[3]{3}} F(\varphi, k) + \sqrt[3]{3} E(\varphi, k) \quad (83)$$

and where the symbols  $F$  and  $E$  denote the incomplete elliptic integrals of the first and second kind, whose argument  $\varphi$  and parameter  $k$  are defined as

$$\left. \begin{aligned} \varphi &= \arccos \frac{\sqrt{3} - 1 + \sqrt[3]{4\eta^2(1 - \eta^2)}}{\sqrt{3} + 1 - \sqrt[3]{4\eta^2(1 - \eta^2)}} \\ k &= \sqrt{(2 + \sqrt{3})/4} \end{aligned} \right\} \quad (84)$$

The thickness ratio of this body of revolution and the associated drag coefficient are given by

$$\tau = 1.596\sqrt{V/l^3}, \quad C_D = 0.321\tau^2 \quad (85)$$

### (6.6) Given Wetted Area and Volume

If the wetted area and the volume are prescribed while the length and the thickness are free, the transversality condition leads to  $K_1 = 0$ ,  $K_2 + K_3 = 0$ . Consequently, solution of the transition equation yields the following coordinates for the transition point:

$$\xi_0 = 0.463, \quad \eta_0 = 0.637 \quad (86)$$

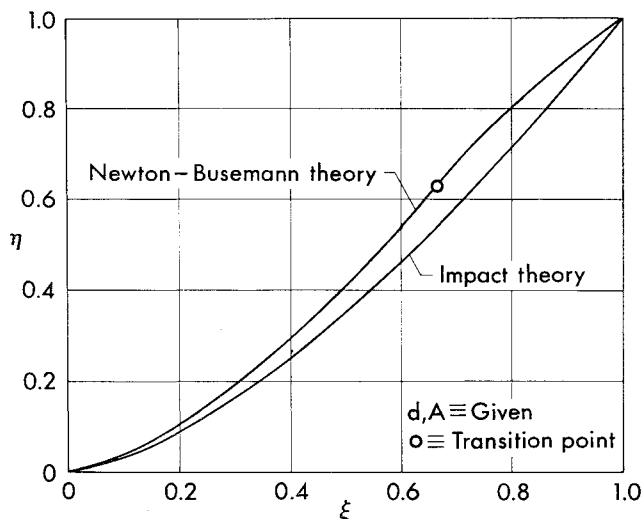


FIG. 3. Comparison of extremal solutions obtained including and neglecting centripetal acceleration effects (given thickness).

The regular shape minimizing the drag is described by the relationship

$$\frac{\xi}{\xi_0} = \frac{1 - (1 - \eta)^{2/3}}{1 - (1 - \eta_0)^{2/3}} \quad (87)$$

The thickness ratio and the drag coefficient are given by

$$\tau = 54.45(V^2/S^3), \quad C_D = 0.307\tau^2 \quad (88)$$

## (7) Discussion of Results

From the previous analysis, it appears that, despite the generality of this problem, the present method is relatively simple and has the merit of leading to analytical solutions in each of the twelve particular cases considered here. The main comments to these solutions are as follows:

(a) For problems where the thickness is given, the extremal arc consists of a power body followed by a free layer, with the transition point in the second half of the body. In the two-dimensional case, the exponent of the power body is 1 if the length is given, 3/2 if the enclosed area is given, and 3 if the moment of inertia of the contour is given; the transition point is at 50 percent of the length if the length is given, at 66 percent if the enclosed area is given, and at 83 percent if the moment of inertia of the contour is given. In the axisymmetric case, the exponent of the power body is 3/4 if the length is given, 1 if the wetted area is given, and 3/2 if the volume is given; the transition point is at 60 percent of the length if the length is given, at 70 percent if the wetted area is given, and at 80 percent if the volume is given. It is of interest to compare the present shapes with those obtained by means of the simple impact theory.<sup>1,2</sup> The latter theory excludes the possibility of a free layer and predicts that the entire extremal arc is a power body of exponent identical to that determined here. With reference to the two-dimensional solution minimizing the drag for a given thickness and a given enclosed area, this comparison is shown in Fig. 3 and indicates that the extremal arc calculated with the Newton-Busemann pressure coefficient law is always more blunt than the extremal arc calculated using Newton's impact theory.

(b) For problems where the thickness is free, the extremal arc is composed of a regular shape and a free layer; however, the equation governing the regular shape is not that of a power body; furthermore, the transition point is located in the first half of the body. In the two-dimensional case, the transition point is at 28 percent of the length if the length and the enclosed area are given, at 32 percent if the length and the moment of inertia of the contour are given, and at 45 percent if the enclosed area and the moment of inertia of the contour are given. In the axisymmetric case, the transition point is at 35 percent of the length if the length and the wetted area are given, at 39 percent if the length and the volume are given, and at 46 percent if the wetted area and the volume are given. Compari-

son of the present solutions with those derived from the impact theory shows that corresponding extremal arcs cross at some point in the second half of the body (see Fig. 4, for a particular example relative to the two-dimensional solution minimizing the drag for a given length and a given enclosed area). Specifically, the extremal arc calculated with the Newton-Busemann pressure coefficient law is more blunt than the extremal arc calculated using Newton's impact theory in the region of the leading edge.

(c) An interesting difference between two-dimensional and axisymmetric solutions is that the slope of the extremal arc at the initial point is always finite in the two-dimensional case, while it is infinite in those axisymmetric problems where the length is prescribed. It follows that the slender body approximation  $\dot{y}^2 \ll 1$  is never violated in the two-dimensional case, providing that  $\tau^2 \ll 1$ , where  $\tau$  is the thickness ratio. On the other hand, the slender body approximation may be violated locally in the axisymmetric case: this occurs in the region which immediately surrounds the nose of the optimum body if the boundary conditions are such that the length of the body is prescribed. However, if one defines the critical region as the region identified by the inequality  $\dot{y} \geq \tau$ , it is possible to show that the contribution of this region to the overall drag is small and can be neglected for practical engineering applications.<sup>1, 2</sup> For these reasons, the shape predicted using the slender body approximation is very close to the shape which can be obtained without using this approximation.

(d) Regardless of the boundary conditions, all of the extremal solutions presented here are discontinuous in the curvature. This discontinuity occurs at the transition point between the regular shape and the free layer and causes a discontinuity in the centripetal acceleration and, hence, in the pressure coefficient. In this connection, the writer emphasizes that the basic reason for these discontinuities does not lie in the variational procedure employed here, but rather in the formula employed for the distribution of pressure coefficients, that is, the Newton-Busemann law: the latter forecasts a discontinuity in the pressure coefficient for those shapes which have a discontinuity in the radius of curvature.

(e) It is remarked that, since the present solutions are continuous in the slopes, they belong to the class of problems defined by Hayes and Probstein as proper optimum problems.<sup>6</sup> No attempt has been made to investigate the class of absolute optimum problems in which a discontinuity in the slope is allowed by using a so-called thrust cowl.

(f) In order to control the correctness of the results obtained, as well as to evaluate the relative advantage or disadvantage of one variational solution with respect to another, systematic numerical analyses have been carried out in Refs. 3 and 4. As an example of the two-dimensional type, the wedge-free layer solution exhibits 25 percent less drag than the 3/2-power body-

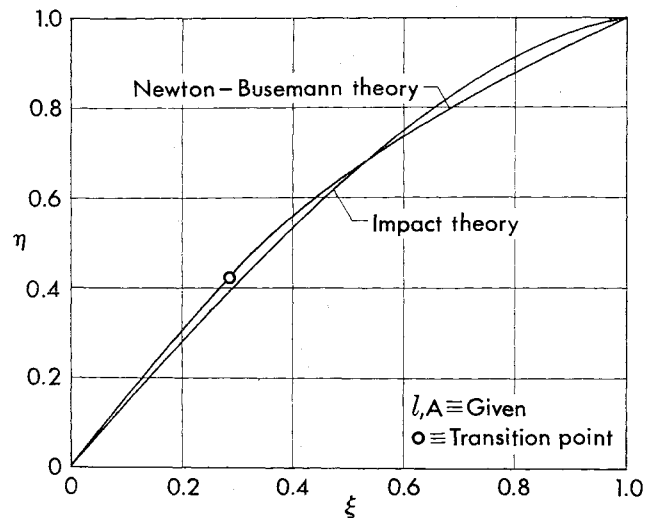


FIG. 4. Comparison of extremal solutions obtained including and neglecting centripetal acceleration effects (free thickness).

free layer solution having the same thickness and length however, the drag of the latter is about 12 percent less than the drag of the former if the comparison is made for the same thickness and enclosed area. As an example of the axisymmetric type, the 3/4-power body-free layer solution exhibits 15 percent less drag than the cone-free layer solution having the same thickness and length; however, the drag of the latter is about 9 percent less than the drag of the former if the comparison is made for the same thickness and wetted area.

(g) In Refs. 3 and 4, a systematic comparison has been carried out between the present variational solutions and the optimum power bodies. As an example of the two-dimensional type, the extremal solution for given thickness and length yields 16 percent less drag than the optimum power body (Ref. 4); furthermore, the extremal solution for given length and enclosed area yields 29 percent less drag than the optimum power body. As an example of the axisymmetric type, the extremal solution for given thickness and length yields 14 percent less drag than the optimum power body;<sup>4</sup> furthermore, the extremal solution for given length and wetted area yields 28 percent less drag than the optimum power body.

## References

- <sup>1</sup> Miele, A., *Optimum Slender, Two-Dimensional Bodies in Newtonian Flow*, Boeing Scientific Research Labs., Flight Sciences Lab., TR No. 60, 1962.
- <sup>2</sup> Miele, A., *Optimum Slender Bodies of Revolution in Newtonian Flow*, Boeing Scientific Research Labs., Flight Sciences Lab., TR No. 56, 1962.
- <sup>3</sup> Miele, A., *A Study of the Slender Two-Dimensional Body of Minimum Drag Using the Newton-Busemann Pressure Coefficient Law*, Boeing Scientific Research Labs. Flight Sciences Lab., TR No. 61, 1962.
- <sup>4</sup> Miele, A., *A Study of the Slender Body of Revolution of Minimum Drag Using the Newton-Busemann Pressure Coefficient Law*, Boeing Scientific Research Lab., Flight Sciences Lab. TR No. 62, 1962.

(Continued on page 195)

## References

- <sup>1</sup> Schiller, L., *Die Entwicklung der Laminaren Geschwindigkeitsverteilung und ihre Bedeutung für Zähigkeitsmessungen*, ZAMM, Vol. 2, p. 96, 1922.
- <sup>2</sup> Boussinesq, J., *Sur la manière dont les vitesses, dans un tube cylindrique de section circulaire, évasé à son entrée, se distribuent depuis celle entrée jusqu'aux endroits où l'on trouve établi un régime uniforme*, Comptes Rendus, Vol. 113, pp. 9-15, 49-51, 1891.
- <sup>3</sup> Rivas, Miguel A., Jr., and Shapiro, Ascher H., *On the Theory of Discharge Coefficients for Round-Entrance Flowmeters and Venturis*, Trans. ASME, Vol. 78, No. 3, pp. 489-497, April 1956.
- <sup>4</sup> Simmons, Frederick S., *Analytical Determination of Discharge Coefficients for Flow Nozzles*, NACA TN 3449, 1955.
- <sup>5</sup> Maslen, Stephen H., *On Fully Developed Channel Flows: Some Solutions and Limitations, and Effects of Compressibility, Variable Properties, and Body Forces*, NASA TR R-34, 1959.
- <sup>6</sup> Martin, Dale E., *A Study of Laminar Compressible Viscous Pipe Flow Accelerated by a Body Force, with Application to Magnetogasdynamics*, NASA TN D855, April 1961.
- <sup>7</sup> Henshal, Brian D., and Zlotnic, Martin, *Design Study for a Hypersonic Low Density Wind Tunnel*, Research and Advanced Development Div., Avco Corp., Tech. Rep., RAD-TR-9-60-37, Jan. 31, 1961.
- <sup>8</sup> Sutton, George P., *Rocket Propulsion Systems for Interplanetary Flight*, Journal of the Aero/Space Sciences, Vol. 26, No. 10, Oct. 1959.
- <sup>9</sup> Pai, Shih I., *Viscous Flow Theory, Volume 1 Laminar Flow*, 1st Ed., D. Van Nostrand Company, Inc., Princeton, N. J., 1956.
- <sup>10</sup> Williams, James C. III, *A Study of Compressible and Incompressible Viscous Flow in Slender Channels*, Ph.D. Thesis, University of Southern California, June 1962.
- <sup>11</sup> Byrd, Paul F., and Friedman, Morris D., *Handbook of Elliptic Integrals for Engineers and Physicists*, Springer-Verlag, Berlin, 1954.
- <sup>12</sup> Spencley, G. W., and Spencley, R. M., *Smithsonian Elliptic Functions Tables*, Smithsonian Institution, Washington, D. C., Nov. 1, 1947.
- <sup>13</sup> Millsaps, Knox, and Pohlhausen, Karl, *Thermal Distribution in Jeffery-Hamel Flows Between Nonparallel Plane Walls*, Journal of the Aeronautical Sciences, Vol. 20, No. 3, March 1953.

\* \* \*

## Slender Shapes of Minimum Drag

(Continued from page 178)

- <sup>5</sup> Cole, J. D., *Newtonian Flow Theory for Slender Bodies*, Journal of the Aeronautical Sciences, Vol. 24, No. 6, June 1957.
- <sup>6</sup> Hayes, W. D. and Probstein, R. F., *Hypersonic Flow Theory*, Academic Press, New York, 1959.
- <sup>7</sup> Chernyi, G. G., *Introduction to Hypersonic Flow*, Academic Press, New York, 1961.
- <sup>8</sup> Gonor, A. L., *Determination of the Shape of a Body of Minimum Drag at Hypersonic Speed*, PMM, Vol. 24, No. 6, 1960.
- <sup>9</sup> Bliss, G. A., *Lectures on the Calculus of Variations*, The University of Chicago Press, Chicago, 1946.
- <sup>10</sup> Miele, A., *The Calculus of Variations in Applied Aerodynamics and Flight Mechanics*, Boeing Scientific Research Labs., Flight Sciences Lab., TR No. 41, 1961.
- <sup>11</sup> Miele, A., (Editor), *Extremal Problems in Aerodynamics*, Academic Press, New York, 1963.

\* \* \*